

# Atomic Force Microscopy Study of Organic–Inorganic Hybrid Materials

Yen Wei,<sup>\*,†</sup> Danliang Jin,<sup>†</sup> Daniel J. Brennan,<sup>‡</sup> Dimaries Nieves Rivera,<sup>†</sup>  
Qing Zhuang,<sup>‡</sup> N. John DiNardo,<sup>\*,‡</sup> and Kunyuan Qiu<sup>§</sup>

Department of Chemistry and Department of Physics and Atmospheric Science,  
Drexel University, Philadelphia, Pennsylvania 19104, and College of Chemistry,  
Peking University, Beijing 100871, China

Received July 10, 1997

A series of monolithic poly[methyl methacrylate-*co*-3-(trimethoxysilyl)propyl methacrylate]–silica hybrid materials have been prepared via the sol–gel reactions. The fracture surfaces of the materials were systematically examined with atomic force microscopy (AFM) as a function of the silica content from ~23 to 100 vol %. For the transparent materials, the AFM image of the sample at a low silica content of 23 vol % is very smooth and essentially featureless while those at higher silica contents show relatively greater surface roughness and development of domains of various shapes and sizes. In sharp contrast, the optically translucent and phase-separated samples exhibit significantly higher surface roughness and larger domain size than all the transparent hybrid materials, suggesting that the transparent materials might have little or no organic–inorganic phase separation.

## Introduction

There is considerable interest in organic–inorganic hybrid/composite materials prepared via the sol–gel process.<sup>1–3</sup> A variety of organic polymers have been introduced into inorganic networks to afford the hybrid or composite materials with or without covalent bonding between the polymer and inorganic components, respectively.<sup>1–11</sup> The sol–gel reactions are known to be affected by many synthetic parameters such as structure and concentration of the reactants, solvents, and catalysts as well as reaction temperature and rate of removal of byproducts and solvents.<sup>12,13</sup> In particular,

the presence of organic components modifies the morphology and physical properties of the sol–gel products. For example, the base-catalyzed sol–gel reactions usually result in translucent or opaque products with visible organic–inorganic phase separation. Under acid catalysis and carefully controlled reaction conditions, transparent and monolithic hybrid/composite materials can be obtained.

Recently, we have synthesized a family of monolithic and transparent hybrid materials via the acid- or photoacid-catalyzed sol–gel reactions of inorganic precursors such as tetraethyl orthosilicate (TEOS) with polymer precursors that contain reactive alkoxy-silyl groups.<sup>9–11</sup> A key issue that remains unresolved in these organic-modified materials is the degree of mixing of the organic–inorganic components, i.e., the phase homogeneity. The high optical transparency to visible light indicates that the organic–inorganic phase separation, if any, is on a scale of  $\leq 400$  nm. Many conventional methods for analyzing composite materials have not proven to be effective. For example, the changes in and disappearance of well-defined glass transition of the polymer component as measured by differential scanning calorimetry (DSC) or dynamic mechanical analysis

\* To whom correspondence should be addressed.

<sup>†</sup> Department of Chemistry, Drexel University.

<sup>‡</sup> Department of Physics and Atmospheric Science, Drexel University.

<sup>§</sup> Peking University.

(1) Mark, J. E.; Lee, C. Y.-C.; Bianconi, P. A., Eds. *Hybrid Organic–Inorganic Composites* (*Am. Chem. Soc. Symp. Ser. 585*); American Chemical Society: Washington, D.C., 1995.

(2) (a) Wilkes, G. L.; Huang, H.; Glaser, R. H. In *Silicon-Based Polymer Science* (*Advances in Chemistry Series 224*); Ziegler, J. M., Fearon, F. W., Eds.; American Chemical Society: Washington, D.C., 1990; p 207. (b) Novak, B. M. *Adv. Mater.* **1993**, *5*, 422. (c) Calvert, P. *Nature* **1991**, *353*, 501.

(3) (a) Wen, J.; Wilkes, G. L. *Chem. Mater.* **1996**, *8*, 1667. (b) Frisch, H. L.; Mark, J. E. *Chem. Mater.* **1996**, *8*, 1735.

(4) (a) Mark, J. E.; Pan, S. *Makromol. Chem., Rapid Commun.* **1982**, *3*, 681. (b) Brennan, A. B.; Wilkes, G. L. *Polymer* **1991**, *32*, 733. (c) Haruvy, Y.; Webber, S. E. *Chem. Mater.* **1991**, *3*, 501.

(5) David, I. A.; Scherer, G. W. *Chem. Mater.* **1995**, *7*, 1957.

(6) Saegusa, T. *Macromol. Symp.* **1995**, *98*, 719.

(7) (a) Landry, C. J. T.; Coltrain, B. K.; Wesson, J. A.; Zumbulyadis, N.; Lippert, J. L. *Polymer* **1992**, *33*, 1486. (b) Fitzgerald, J. J.; Landry, C. J. T.; Pochan, J. M. *Macromolecules* **1992**, *25*, 3715.

(8) (a) Huang, H.-H.; Orler, B.; Wilkes, G. L. *Macromolecules* **1987**, *20*, 1322. (b) Parkhurst, C. S.; Doyle, W. F.; Silverman, L. A.; Singh, S.; Andersen, M. P.; McClurg, D.; Wnek, G. E.; Uhlmann, D. R. *Mater. Res. Soc. Symp. Proc.* **1986**, *73*, 769.

(9) Wei, Y.; Bakthavatchalam, R.; Whitecar, C. K. *Chem. Mater.* **1990**, *2*, 337.

(10) Wei, Y.; Yang, D.; Bakthavatchalam, R. *Mater. Lett.* **1992**, *13*, 261.

(11) (a) Wei, Y.; Wang, W.; Yeh, J.-M.; Wang, B.; Yang, D.; Murray, J. K., Jr. *Adv. Mater.* **1994**, *6*, 372. (b) Wei, Y.; Yeh, J.-M.; Jin, D.; Jia, X.; Wang, J. *Chem. Mater.* **1995**, *7*, 969. (c) Wei, Y.; Yang, D.; Tang, L.; Hutchins, M. K. *J. Mater. Res.* **1993**, *8*, 1143. (d) Wei, Y.; Yang, D.; Tang, L. *Makromol. Chem., Rapid Commun.* **1993**, *14*, 273. (e) Wei, Y.; Wang, W.; Yang, D.; Tang, L. *Chem. Mater.* **1994**, *6*, 1737. (f) Wei, Y.; Jin, D.; Yang, C.; Wei, G. *J. Sol-Gel Sci. Technol.* **1996**, *7*, 199. (g) Wei, Y.; Wang, W.; Jin, D.; Yang, D.; Tartakovskaya, L. *J. Appl. Polym. Sci.* **1996**, *64*, 1893. (h) Huang, Z. H.; Qiu, K. Y.; Wei, Y. *J. Polym. Sci. A: Polym. Chem.* **1997**, *35*, 2403.

(12) Brinker, C. J.; Scherer, G. W. *Sol–Gel Science, the Physics and Chemistry of Sol–Gel Processing*; Academic Press: San Diego, 1989.

(13) (a) Mackenzie, J. D., Ulrich, D. R., Eds. *Ultrastructure Processing of Advanced Ceramics*; Wiley: New York, 1988. (b) Klein, L. C. *Sol–Gel Technology*; Noyes Publications: Park Ridge, N. J., 1988. (c) Hench, L. L.; West, J. K. *Chem. Rev.* **1990**, *90*, 33.

**Table 1. Organic–Inorganic Composition and AFM Parameters Measured in the Range of 2000 nm of the Hybrid Materials Derived from the HCl-Catalyzed Sol–Gel Reactions of Tetraethyl Orthosilicate with Poly[methyl methacrylate-*co*-3-(trimethoxysilyl)propyl methacrylate]**

sample code	appearance <sup>a</sup>	silica content			density ( $d$ ), g/cm <sup>3</sup>	AFM average roughness, Å
		wt % calc <sup>b</sup>	wt % expt <sup>c</sup>	vol % <sup>d</sup>		
PMS30	transparent	33.2	32	23	1.328	4.5
PMS30P	translucent	33.2	32	23	1.328	274.9
PMS50	transparent	52.3	52	41	1.422	85.0
PMS80	transparent	80.9	77	69	1.669	45.9
sol–gel silica	transparent	100.0	>98	>98	1.850	83.2

<sup>a</sup> Transparent samples exhibit ~90% of transmittance in the visible wavelength range as determined by optical spectroscopy. <sup>b</sup> Calculated from the reactant stoichiometry. <sup>c</sup> Experimentally determined from the TGA measurements at 750 °C under air. <sup>d</sup> Vol % = wt % ( $d_{\text{hybrid}}/d_{\text{silica}}$ ), where  $d_{\text{silica}} = 1.85 \text{ g/cm}^3$ .

(DMA) suggest the diminution of phase separation but offer little quantitative information.<sup>5,7,9</sup> Transmission electron microscopy (TEM) often fails to provide useful morphological data because of weak contrast.<sup>5</sup> Recently, there have been several reports with encouraging examples of applying atomic force microscopy (AFM) in the analysis of sol–gel materials.<sup>5,6</sup>

In this article, we present a systematic AFM study of the morphology of fracture surfaces of monolithic poly-methacrylate–silica hybrid materials prepared with various organic–inorganic compositions and reaction conditions. The microscopic morphological features such as grain size and roughness are examined in relation to the chemical compositions and optical properties of the hybrid materials.

### Experimental Section

The polymer precursor, i.e., poly[methyl methacrylate-*co*-3-(trimethoxysilyl)propyl methacrylate] [poly(MMA-*co*-MSMA)], was synthesized by free-radical copolymerization of 3-(trimethoxysilyl)propyl methacrylate (MSMA) with methyl methacrylate (MMA) using benzoyl peroxide as initiator in benzene at 60 °C.<sup>10</sup> The copolymer contained 10 mol % of MSMA units and had a number-average molecular weight of 83 600 as determined with gel-permeation chromatography calibrated with polystyrene standards. The hybrid materials were prepared following the previously reported general procedures.<sup>9,10</sup> A 10 wt % solution of poly(MMA-*co*-MSMA) in tetrahydrofuran (THF) was prepared as Sol A. TEOS was prehydrolyzed for 2 h at 60–80 °C in the mixture of THF, water, and 2 M HCl at a [TEOS]:[THF]:[H<sub>2</sub>O]:[HCl] molar ratio of 1:3:3:0.01 to afford Sol B. On the basis of the desired hybrid compositions, appropriate amounts of Sol A and Sol B were mixed under stirring to give homogeneous solutions, which were cast in molds and allowed to undergo gelation and drying at room temperature. After about 2–3 weeks, transparent and colorless hybrid materials were obtained as monolithic disks (20 mm in diameter and 4 mm in thickness). For comparison, a phase-separated sample (PMS30P) was intentionally prepared as a monolithic but translucent disk by accelerating the gelation and drying process ( $\leq 1$  week). A pure sol–gel silica sample was also prepared from Sol B alone.

The AFM measurements were performed on fresh fracture surfaces of the samples with a Digital Instruments Nanoscope III atomic force microscope in contact mode with the standard silicon nitride (Si<sub>3</sub>N<sub>4</sub>) probe tips.<sup>14</sup> Thermogravimetric analysis (TGA) was performed on a TA System 2200 equipped with a TGA 950 module under air atmosphere at a heating rate of 10 °C/min in a temperature range of 25–950 °C.<sup>9</sup> Brunauer–Emmett–Teller (BET) surface area and pore volume<sup>15</sup> were determined by nitrogen adsorption–desorption isotherm measurements on a Micromeritics ASAP2010 micropore analyzer. Each sample was ground into a fine powder of <25  $\mu\text{m}$  in

diameter and was degassed overnight at 473 K and 10<sup>−6</sup> Torr before measurement. Optical transparency was measured on a Perkin-Elmer Lambda 9 UV–vis spectrophotometer.

### Results and Discussion

The compositions, i.e., percentage silica contents by weight (wt %) of the hybrid materials were determined by TGA and the values are comparable to those calculated from the reactant stoichiometry as listed in Table 1. The corresponding silica contents by volume (vol %) were also obtained from the values in wt % and the bulk density of the samples, measured using Archimede's method with water as the medium at 25.0 °C. TEM and X-ray diffraction (XRD) studies failed to yield useful information. Both TEM images at magnifications up to  $5 \times 10^5$  and small-angle XRD patterns of the transparent samples were featureless. The wide-angle XRD patterns consisted of a typical amorphous halo. Usually inorganic materials prepared from sol–gel process without sintering have a microporous structure with a relatively high surface area.<sup>12</sup> Indeed, the BET surface area<sup>15</sup> of pure sol–gel silica was found to be 77 m<sup>2</sup>/g with a pore volume of ~0.05 cm<sup>3</sup>/g. In contrast, all the hybrid materials, regardless of the compositions, exhibit very small BET surface areas (1–3 m<sup>2</sup>/g) and pore volumes (~0.005 cm<sup>3</sup>/g). The values are close to those for fused silica (~1 m<sup>2</sup>/g and 0.002 cm<sup>3</sup>/g) with bulk density of 2.19 g/cm<sup>3</sup>. These observations suggest that the introduction of polymethacrylate chains significantly reduces the pore formation in the sol–gel process.

The fresh fracture surfaces were prepared by breaking the monolithic samples immediately prior to the measurements. In general, the topographic features obtained with AFM were found to depend on the organic–inorganic composition and optical transparency. Figure 1 shows two representative topographic views of the materials. At a low silica content (i.e., 23 vol %), the transparent sample PMS30 (Figure 1a) exhibits a smooth, random, and relatively featureless surface. In sharp contrast, the translucent sample, i.e., PMS30P (Figure 1b), shows clearly discernible grain domains of much greater dimensions (~570 nm in average diameter) although the silica content in PMS30P is identical to that in the transparent sample PMS30 (Figure 1a). This is consistent with the observed optical transparency because the lack of transparency in PMS30P can

(14) DiNardo, N. J. *Nanoscale Characterization of Surfaces and Interfaces*; VCH: Weinheim, 1994.

(15) (a) Sing, K. S. W.; Everett, D. H.; Haul, R. A. W.; Moscou, L.; Pierotti, R. A.; Rouqu  rol, J.; Siemieni  wska, T. *Pure Appl. Chem.* **1985**, *57*, 603. (b) Lowell, S. *Introduction to Powder Surface Area*, John Wiley and Sons: New York, 1979. (c) Lippens, B. C.; de Boer, J. H. J. *Catal.* **1965**, *4*, 319.

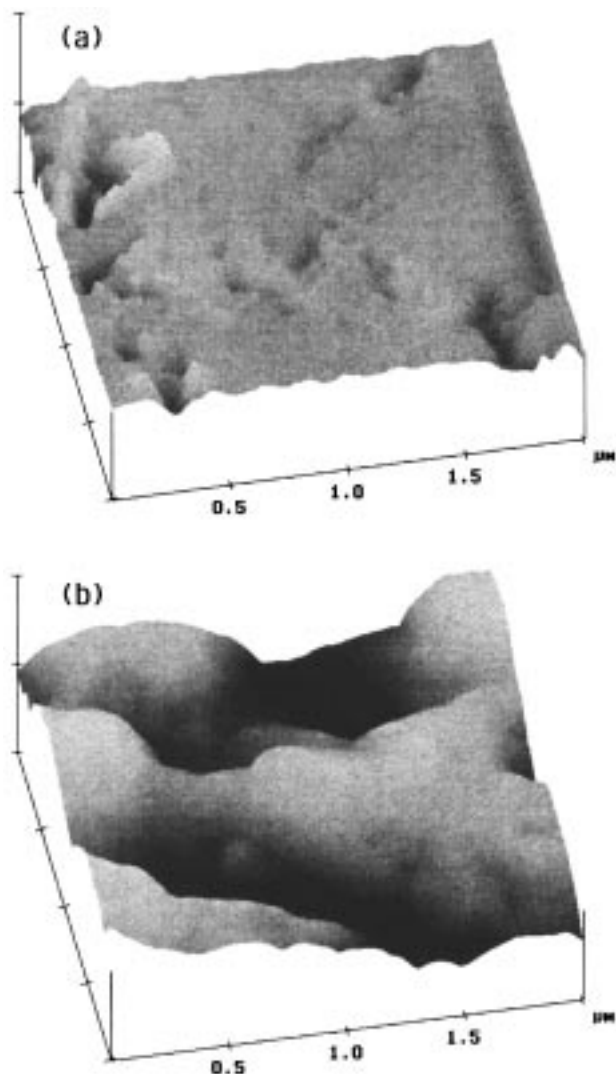


**Figure 1.** AFM topographic views ( $2\ \mu\text{m} \times 2\ \mu\text{m}$ ) of the fracture surfaces of (a) transparent PMS30 ( $Z$  scale: 10 nm/division) and (b) translucent PMS30P ( $Z$  scale: 150 nm/division).

be attributed to the organic–inorganic phase separation at large scales (i.e.,  $\geq 400\ \text{nm}$ ) as confirmed qualitatively by DSC studies.<sup>9,10</sup> At higher silica contents, the transparent samples PMS50 and PMS80 containing 41 and 69 vol % of silica, respectively, appear to have assemblies of grain domains with sizes being much smaller than those in PMS30P (Figure 1b). The morphological characteristics are also reflected in the surface roughness values. As listed in Table 1, the average roughness of the translucent PMS30P (275 Å) is about 50 times greater than that of the transparent PMS30 (5 Å) in the identical measurement range of 2000 nm. The samples with higher silica contents (i.e., PMS50, PMS80, and pure silica) have roughness values of  $\sim 50$  to 90 Å, which are greater than those for PMS30 but still significantly lower than those for the translucent PMS30P. The same trend was observed in other measurement ranges from 500 to 12 000 nm. Though the organic or inorganic component could not be distinctly identified from the AFM images, all the results suggest that the transparent polymethacrylate–silica hybrid materials have little or no organic–inorganic phase separation.

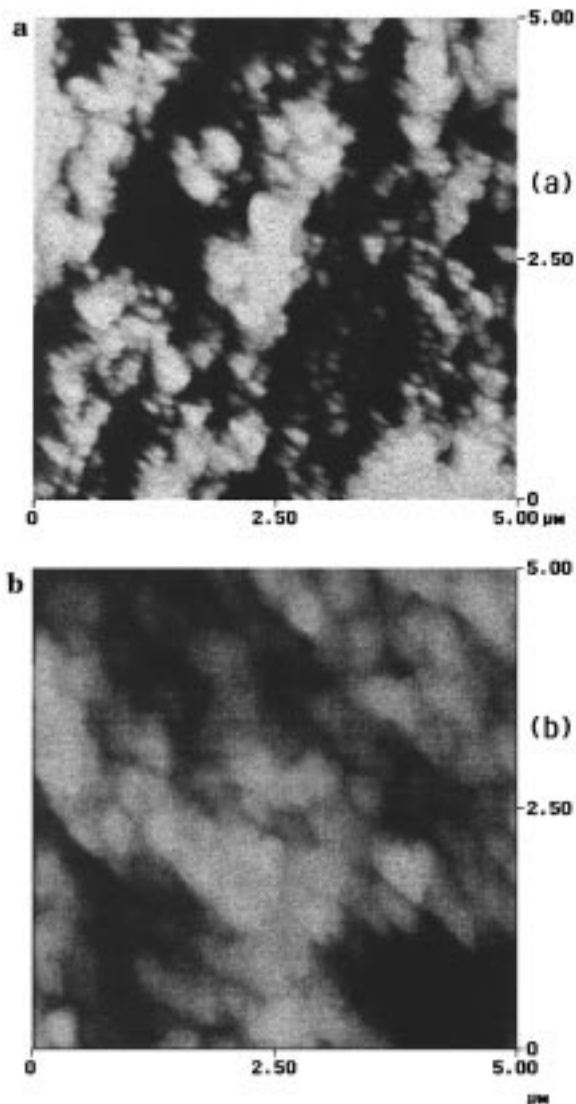


**Figure 2.** AFM top views ( $5\ \mu\text{m} \times 5\ \mu\text{m}$ ) of the fracture surfaces of (a) PMS50 and (b) PMS80.

It is interesting to note that the structures with similar grain domain size and shape appear to be evenly distributed in the AFM top-view images of PMS50 and PMS80 at various magnifications. In PMS50 (Figure 2a) the average domain size is  $\sim 170\ \text{nm}$  with somewhat oval shape, while in PMS80 (Figure 2b) the domains are relatively larger (average  $\sim 250\ \text{nm}$ ). The image of pure sol–gel silica resembles that of PMS50 and has a domain size of  $\sim 120\ \text{nm}$ . Such a domain structure is not related to the micropores in the sol–gel silica because its pore size is smaller than 15 Å as determined by the nitrogen adsorption–desorption isotherm measurements. The formation of the domain structure could be attributed to the development of microcolloidal particulation during the sol–gel reactions.<sup>12</sup> We believe that this mechanism would also be applicable to the transparent polymer–silica hybrid systems. Thus, both the polymer and silica components could exist in each domain, in which the chains of one component are entwined with those of the other intimately through the covalent bonding. When the organic polymer is dominant (e.g., in PMS30), the continuous phase is the polymer matrix, which “traps” the silica components at molecular level via the covalent bonding with little or

no silica particulation. This could explain the observed high homogeneity in the AFM images of PMS30. As the silica content is increased to 41 vol % in PMS50, the organic polymer chains tend to cover the surface of silica colloidal particles to lower the surface energy of the particles during the sol-gel reactions, resulting in the observed domains. At even higher silica content, i.e., 69 vol % in PMS80, fewer polymer chains are available to cover the silica particles so that the silica particles and, hence, domain size become greater than those in PMS50. Further investigation is in vigorous progress to test this hypothesis with AFM and other surface characterization techniques.<sup>14</sup>

In summary, a series of monolithic polymethacrylate-silica hybrid sol-gel materials have been prepared and their fracture surfaces examined systematically by means of AFM as function of the silica content from ~23 to 100 vol %. The optically translucent, phase-separated sample exhibits significantly higher surface roughness and larger domain size than *all* the transparent hybrid materials, suggesting that the transparent materials

might have little or no organic-inorganic phase separations. For the transparent materials, the AFM image of the sample at a low silica content (i.e., 23 vol %) is very smooth and essentially featureless while those at higher silica contents show relatively greater surface roughness and development of domains of various shapes and sizes. A preliminary model related to the silica colloidal particulation has been postulated to rationalize the observations.

**Acknowledgment.** This work has been supported by National Institutes of Health (Grant No. DE09848 to Y.W.) and by National Natural Science Foundation of China (Grant No. 29710110-780 to K.Q. and Y.W.). We thank Drs. B. Jiang and C. Chen for some of TEM, XRD, and neutron scattering measurements. We are grateful to the referees of this article for helpful suggestions. D.N.R. acknowledges support from the NSF-REU program.

CM970703O